Journal of Chemistry and Technologies, 2026, *34*(2), 439-447

Journal of Chemistry and Technologies

pISSN 2663-2934 (Print), ISSN 2663-2942 (Online).

journal homepage: http://chemistry.dnu.dp.ua
editorial e-mail: chem.dnu@gmail.com

UDC 502.131.1:628.4.032:663.93:66.081

THERMAL ANALYSIS AND IR SPECTROSCOPY OF COFFFEE GROUNDS AND COFFEE-GROUND-DERIVED BIOCHARS

Galyna Krusir[1,2], Myroslav Malovanyy[3], Viktoria Kochubei[3], Heinz Leuenberger[2], Serhii Moshtakov[2], Taisiia Sokolova[4], Tatyana Shpyrko[1]

[1] Odesa National Technological University, St. Kanatna, 112, Odesa, Ukraine, 65039
[2] Institute for Ecopreneurship, School of Life Sciences, University of Applied Sciences and Arts Northwestern Switzerland, Hofackerstrasse 30, 4132 Muttenz, Switzerland
[3] Lviv Polytechnic National University, Stepana Bendery 12, Lviv, Ukraine, 79000
[4]National Technical University "Kharkiv Polytechnic Institute" 2, Kyrpychova St., Kharkiv, 61002
Received 9 March 2026; accepted 30 April 2026; available online 20 June 2026

Abstract

The worsening environmental, food and energy crisis necessitates new approaches to recycling food waste into targeted products, one of which is coffee grounds. The produced biochars, featuring a high specific surface area and suitable pore dimensions, are considered relevant and promising for addressing environmental challenges in the waste management sector. The aim of the objective of this research is to produce biochar, which can be used efficiently and effectively in the future during the process of anaerobic digestion of food waste from a hotel and restaurant complex to produce biogas, to study its structural surface characteristics and its physicochemical characteristics using integral and differential infrared spectroscopy and complex thermal analysis. The differential infrared spectrum of the comparison of biochar and feedstocks is characterised by a decrease in the absorption intensity of the feedstock in the 3400 cm-1 region, which corresponds to the valence vibrations of the free OH- group, indicating an increase in hydrogen bonds in biochar. To evaluate the effect of temperature on the thermal decomposition of the samples, a comprehensive thermal analysis was used, including differential thermogravimetry (DTG), thermogravimetric analysis (TG) and differential thermal (DTA) analyses. The less intense mass loss of biochar-300 and biochar-500 samples compared to the samples of the feedstock and biochar-MX confirms the presence of fewer thermally unstable components in them. Compared to the raw material sample, the samples of all the studied biochars contain fewer components capable of thermal oxidation. Structural characteristics of the biochar surface have a significant impact on the functional properties of biochar, the specific surface of biochar is much higher than the specific surface of raw materials, which indicates the feasibility of the selected methods of modifying raw materials to increase their functional properties.

Keywords: complex thermal analysis; spent coffee grounds; biochar; physical and chemical properties; infrared spectroscopy; surface structure characteristics.

ТЕРМІЧНИЙ АНАЛІЗ ТА ІЧ-СПЕКТРОСКОПІЯ КАВОВОЇ ГУЩІ ТА БІОЧАРІВ НА ЇЇ ОСНОВІ

Галина Крусір[1,2], Мирослав Мальований[3], Вікторія Кочубей[3], Хайнц Лойєнбергер[2], Сергій Моштаков[2], Таїсія Соколова[4], Тетяна Шпирко[1]

[1]Одеський національний технологічний університет, вул. Канатна, 112, м. Одеса, Україна, 65039
[2]Інститут екопідприємництва, Школа наук про життя, Університет прикладних наук та мистецтв Північно-Західної Швейцарії, Хофакерштрассе 30, 4132 Муттенц, Швейцарія
[3] Національний університет "Львівська політехніка", вул. Степана Бендери, 12, Львів, Україна, 79000
[4]Національний технічний університет «Харківський політехнічний інститут», вул. Кирпичова, 2, Харків, 61002

Анотація

Поглиблення екологічної, продовольчої та енергетичної криз зумовлює необхідність пошуку нових підходів до перероблення харчових відходів у цільові продукти, одним із яких є кавова гуща. Отримані біовугілля з великою питомою поверхнею та відповідним розміром пор є актуальними й перспективними для розв'язання екологічних проблем у секторі поводження з відходами. Метою цього дослідження є отримання біовугілля, яке в подальшому може бути ефективно використане під час процесу анаеробного зброджування харчових відходів готельно-ресторанного комплексу для виробництва біогазу, а також вивчення його структурних характеристик поверхні та фізико-хімічних властивостей із застосуванням інтегральної та диференціальної інфрачервоної спектроскопії й комплексного термічного аналізу. Диференціальний інфрачервоний спектр порівняння біовугілля та вихідної сировини характеризується зменшенням інтенсивності поглинання вихідного матеріалу в області 3400 см$^{-1}$, що відповідає валентним коливанням вільної групи OH$^-$, і свідчить про збільшення кількості водневих зв'язків у біовугіллі. Для оцінювання впливу температури на термічне

**Corresponding author e-mail: krussir.65@gmail.com*
 doi: 10.15421/jchemtech.v34i2.353798

Journal of Chemistry and Technologies, 2026, *34*(2), 439-447

розкладання зразків було використано комплексний термічний аналіз, який включав термогравіметрію (TG), диференціальну термогравіметрію (DTG) та диференціальний термічний аналіз (DTA). Менша інтенсивність втрати маси зразками біовугілля 300 та біовугілля 500 порівняно з вихідною сировиною та біовугіллям МХ підтверджує наявність у них меншої кількості термічно нестійких компонентів. Порівняно з вихідним матеріалом, усі досліджені зразки біовугілля містять менше компонентів, здатних до термічного окиснення. Структурні характеристики поверхні біовугілля мають істотний вплив на його функціональні властивості: питома поверхня біовугілля є значно більшою, ніж питома поверхня вихідної сировини, що підтверджує доцільність обраних методів модифікації сировини для підвищення її функціональних характеристик.

Ключові слова: комплексний термічний аналіз; відпрацьована кавова гуща; біовугілля; фізико-хімічні властивості; інфрачервона спектроскопія; структурні характеристики поверхні.

Introduction

As a result of the worsening environmental and energy crises observed in recent years, ensuring provision to low-cost, dependable, renewable, and innovative energy options is a priority that will help minimise negative impacts on the environment [1]. A rational approach is to recycle food waste into a secondary product, which accounts for 32 % to 62 % of the total amount of solid household waste, including spent coffee grounds (SCG) [2; 3]. Using SCG in the role of a secondary raw material is an effective alternative within the framework of food waste recycling policy to create a secondary product with added value – biochar, which has characteristics similar to activated carbon. Biochar is obtained by thermochemical conversion at temperatures of 300°C under conditions of limited oxygen supply. Variations of traditional pyrolysis and microwave irradiation have shown positive results in studies of the acid-base and ion-exchange properties of biochar obtained in the temperature range from 230 to 500 °C [3; 4]. The selection of optimal pyrolysis conditions is critical for obtaining a product with specified characteristics and properties, for example, using inert gases (helium, argon) or non-inert gases (CO_2, H_2, NH_2) [5; 6].

Due to the presence of hydroxyl, carboxyl and carbonyl groups in biochar, their activation increases selectivity to diverse pollutants that can be sorbed from various solutions, in particular wastewater. For example, one study noted the biochar's strong adsorption capacity from spent coffee grounds, which proved to be an environmentally friendly and highly effective sorbent with a maximum adsorption capacity (Q_{max}) of 175. 84 mg g^{-1} for the dye Reactive Yellow 161 [7].

Thermal decomposition of biochar produced from SCG through both oxidative and inert torrefaction was also analyzed. Both the raw material and biochar exhibited the highest mass loss in the 300–400 °C range, except for biochar prepared at 300 °C, which exhibited a lower mass yield. TG and DTG curves were similar for both media at identical temperatures and exposure times, suggesting that the type of medium had little influence on mass loss. DTA results indicated that the Toffset values for biochar were generally higher, ranging from 487.9 to 563 °C, compared to raw SCG. The thermal decomposition peak for sample T was observed between 324 and 446 °C. [8].

Extensive research focused on investigating the chemical structure of biochar for Cr (VI) ion sorption using IR Fourier spectroscopy. The presence of carboxyl, amino and carbonyl surface groups was detected, as well as a significant decrease in peak intensity ranging from 3408 to 3429 cm^{-1} and about 546 cm^{-1}. The results showed that pure biochar CH and KL removed 74.98 % and 84.78 % of Cr (VI), respectively, from 20 mg l^{-1} aqueous solutions. The obtained biochar-based nanocomposites sorbed significantly more efficiently – 99.83 % and 99.86 %. Therefore, the use of biochar for the removal of Cr (VI) from wastewater, especially in the form of nanocomposites with magnetic iron oxide, coffee husks and catalyst residues, is a highly effective solution for further application [9].

The production of biochar is a relatively simple and reliable process with significant potential for further research into its properties and comparison with activated carbon, despite uncertainty regarding engineering installations [5]. Its use can be implemented in agriculture for soil remediation, wastewater treatment, and increasing biogas yield in anaerobic digestion [10; 11]. For certain adsorption technologies, a promising product is magnetically sensitive biochar obtained using special technologies [12; 13].

The aim of this study is to investigate the structural characteristics of the surface and physicochemical properties of biochar using integral and differential IR spectroscopy and comprehensive thermal analysis.

To meet this objective, the points outlined below need to be addressed:

1) provide a comparative characterisation of the obtained biochar and plant raw materials using complex thermal analysis;

2) to provide a comparative characterisation of

Journal of Chemistry and Technologies, 2026, *34*(2), 439-447

the obtained biochar and plant raw materials using integral and differential IR spectroscopy;

3) to examine the structural characteristics of raw materials and biochar generated via pyrolysis and microwave treatment.

Synthesis methodology and sample examination

Biochar was generated from 40 g of spent coffee grounds employing thermal (temperature 300 and 500 °C, at a rate of 30 ml/min – biochar-300 and biochar-500 samples, respectively) and microwave pyrolysis (temperature 230°C for 15 min – biochar-MX sample). After washing with deionized water, the material was dried at 105 °C for 24 h and stored in an airtight container.

The structural characteristics were studied using a standard vacuum sorption device equipped with a quartz spiral dynamometer (McBen type) at a constant temperature of 25 degrees Celsius. Discrepancies in the height of mercury columns in the measuring tubes of the manometer were recorded using a KM-8 instrument (cathetometer) with a measurement accuracy of no more than 0.5 per cent. During the experiments, the entire apparatus was placed in a protective plexiglass chamber, where the temperature was maintained at a fixed value of 25 °C with minimal deviations of ± 0.2 °C thanks to a specially designed temperature control system. The quantitative characteristic of the sorbed moisture was calculated using the following mathematical expression:

$$Q = \frac{\Delta l}{\Delta L * M}, \qquad (1)$$

where: ΔL represents the elongation of the quartz helix as a function of the sorbent mass; Δl corresponds to the elongation of the quartz helix as a function of the sorbate mass; M is the molecular weight of the sorbate.

When converted into a linear form, the equation of the BET polymolecular sorption isotherm is as follows:

$$\frac{P/Ps}{a(I-P/P_S)} = \frac{I}{a_m * C} + \frac{C-I}{a_m * C} P/P_S, \qquad (2)$$

where: P_S is the saturated vapour pressure at a given temperature; P/P_S is the relative vapour pressure; a is the surface concentration of sorbate; am is the surface concentration of sorbate when all active centres are filled; C is the BET constant.

Was used to calculate the specific surface area of the samples Eq.

$$S_{yg} = a_m * N_A * S_0, \qquad (3)$$

where: N_A is the Avogadro number; S_0 is the cross-sectional area of sorbate (water) molecules, equal to 10.6 A.

Was used to determine the average effective pore radius Eq.

$$S = \frac{v_{max}}{2\, S_{yg}}, \qquad (4)$$

where: v_{max} is the maximum volume of water that is absorbed.

Comprehensive thermal analysis, including thermogravimetry (TG), differential thermal analysis (DTA) and differential thermogravimetry (DTG), was employed to assess the influence of temperature regimes on the thermal decomposition of the materials under study. The study was conducted using a Q-1500 derivative analyser manufactured by Paulika-Paulika-Erdei, which was connected to a personal computer. Heating of the samples in air was carried out up to a maximum temperature of 1000°C. The temperature increase rate was 5°C per minute (5°C·min^{-}). The volume mass of each sample was fixed at 50 mg. Aluminium oxide was used as the reference material (reference substance).

A Perkin Elmer FT-IR Spectrometer Frontier was employed to acquire the IR spectra of the pressed samples (wavelength range 400–4000 cm^{-1}, resolution 4 cm^{-1}) (Fig. 2). The substance (1 mg) and KBr (200 mg) were combined and pressed at a pressure of 7 t/cm^2 for 30 s. The samples of the starting material and biochar were studied using differential IR spectroscopy 32 based on the parameters of relative optical density, which involved the use of a baseline tangent at intervals of 3400-2500 cm^{-1} and 1800–700 cm^{-1}. The maximum absorption point at 1425 cm^{-1}, which is associated with the deformation vibrations of CH groups, was selected as the internal standard [12; 13]. The expected values of relative optical density for 54 the selected absorption peaks (ROD) were calculated as the ratio:

$$ROD = \frac{D_x}{Dst}, \qquad (5)$$

where DX is the optical density of the absorption band under study with wavenumber x; DST is the optical density of the internal standard.

The optical density was calculated by the formula:

$$D = lg \frac{T_0}{Tx}, \qquad (6)$$

where T_0 is the transmittance in % of the point on the baseline; T_X - transmittance in % of the corresponding point of the spectrum.

The differential spectra of the comparison of drug samples were plotted in the coordinates: change in ΔROD as a function of the wavenumber x.

Specialized software was employed to analyze the statistical data collected during the

Journal of Chemistry and Technologies, 2026, *34*(2), 439-447

experiments: R, Prism, Excel, as well as licensed software ACDLabs 6.0 Professional.

Results and Discussion

Food waste is lignocellulosic raw material containing cellulose (315-400°C), hemicellulose (220-315°C) and lignin (160-900°C), which are subject to decomposition within certain temperature ranges [3; 16; 17]. Organic substances present in biomass degrade under conditions of limited oxygen access. The quality and characteristics of the pyrolysis product are influenced by factors such as process temperature, residence time in the reactor, type of biomass used, and heating rate [16; 17]. The results of a comprehensive thermal analysis performed on biochar samples are presented as thermographic images (Fig. 1) and the corresponding Table 3. A comparison of differential thermal analysis (DTA) curves as illustrated in Fig. 2.

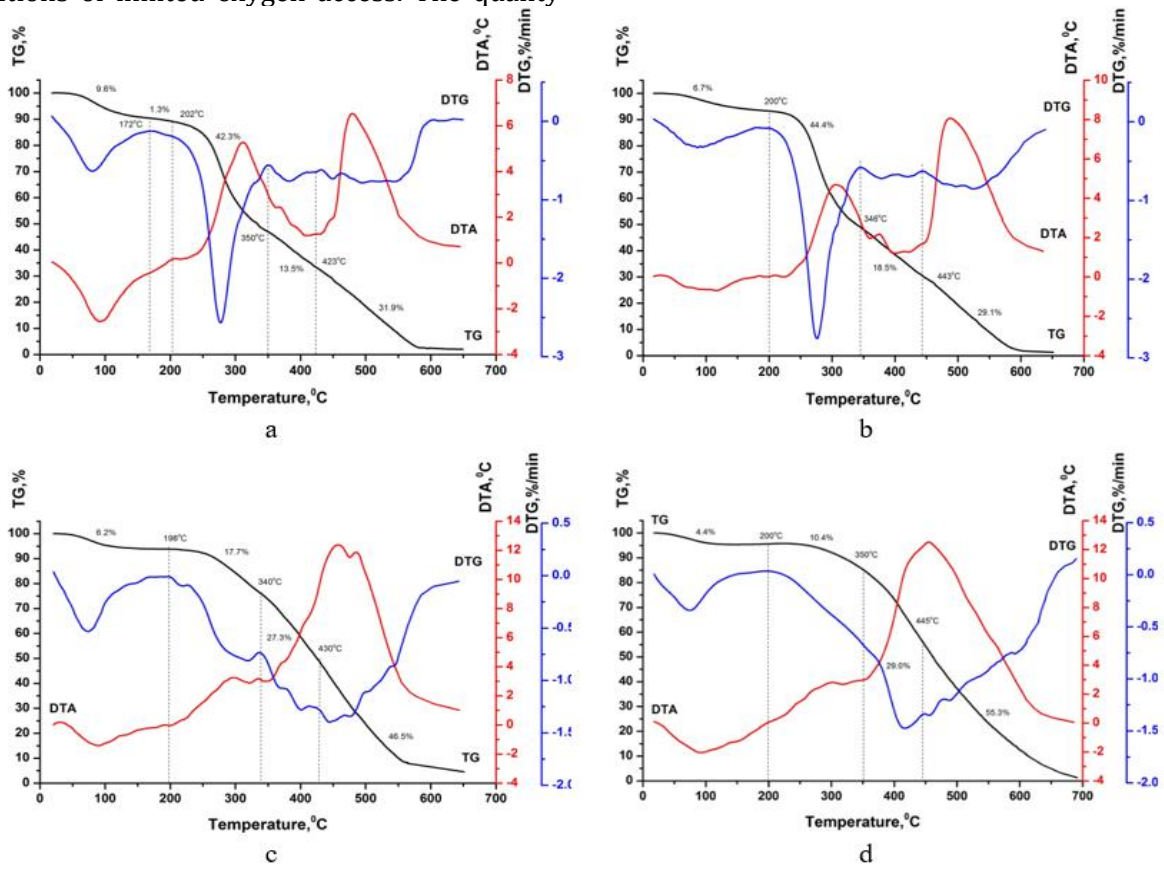

Fig. 1. (a) thermogram of raw materials; (b) thermogram of the biochar-MX obtained using microwave irradiation; (c) thermogram of the Biochar-300; (d) thermogram of the Biochar-500

Table 1

Results of comprehensive thermal analysis of samples

Sample	Stage	Temp. interval [°C]	Weight loss [%]
Raw materials sample 1	I	20–172	9.6
	II	172–202	1.3
	III	202–350	42.3
	IV	350–423	13.5
	V	423–650	31.9
Biochar-MX sample 2	I	20–200	6.7
	II	197–346	44.4
	III	346–443	18.5
	IV	443–650	29.1
Biochar-300 sample 3	I	20–198	6.2
	II	198–340	17.7
	III	340–430	27.3
	IV	430–650	46.5
Biochar-500 sample 4	I	20–200	4.4
	II	200–350	10.4
	III	350–445	29.0
	IV	445–690	55.3

Journal of Chemistry and Technologies, 2026, *34*(2), 439-447

Based on the results of a comprehensive thermal analysis (see Table 1), the first stage of thermal decomposition can be identified, which took place at low temperatures. The initial decrease in the mass of samples, namely: 1 (9.6 %), 2 (6.7 %), 3 (6.2 %), 4 (4.4 %), was caused by the evaporation of adsorbed moisture. This process was recorded by the appearance of peaks on the DTG curves and endothermic dips on the DTA plots.

The second step of thermolysis of the raw material, occurring between 172 and 202 °C, corresponded to the release of water bound to the sample components. During this stage, a slight mass loss of 1.3 % was recorded, accompanied by a shift of the DTA signal toward endothermic behavior [20].

In the temperature interval of 202–350 °C, the raw sample showed a pronounced mass decrease of 42.3 % during the third stage of thermolysis. This loss is attributed to endothermic reactions including hemicellulose pyrolysis, cellulose degradation with a notable shortening of polymer chains and decomposition of lignin. At the same time, the sample components underwent exothermic thermo-oxidation reactions accompanied by sequential combustion of the decomposition products, as evidenced by a distinct exothermic peak on the DTA curve. A clear minimum with the highest value at 277 °C was detected on the DTG curve of the raw material sample [21].

Comparable changes were observed in the biochar-MX, biochar-300 and biochar-500 samples during the second stage of their thermal breakdown. Biochar-MX exhibited a mass loss of 44.4 % between 197 and 346 °C, while biochar-300 lost 17.7% of its mass from 198 to 340 °C and for biochar-500 from 200 to 350 °C it was 10.4 %. These processes were accompanied by exothermic effects on the DTA curves and corresponding extrema on the DTG plots.

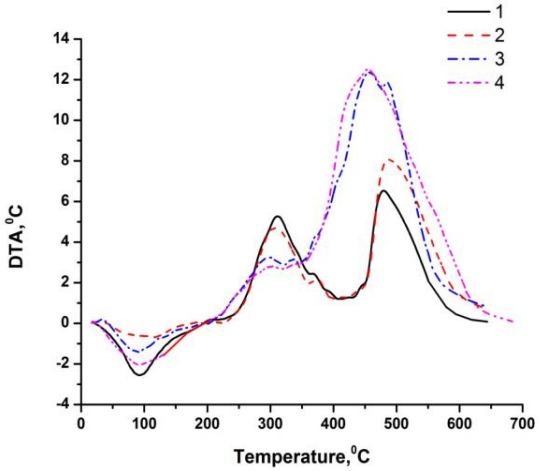

Fig. 2. DTA curves of the samples compared

Differences in mass between the raw material and biochar between 197 and 350 °C indicate the different chemical compositions of these materials. The biochar-300 and biochar-500 samples show less pronounced weight loss relative to the raw material and biochar-MX, which confirms their lower content of thermally unstable substances. Also, in all studied biochar samples, relative to the raw material, fewer components are prone to thermal oxidation. This is evidenced by weaker pronounced exothermic peaks on the DTA curves in the specified temperature range (197–350 °C) (see Fig. 2). At the fourth stage of thermal decomposition, in the temperature range of 350–423 °C, the raw material gradually lost mass (by 13.5 %). This corresponded to the burning of the remains of its destruction, as evidenced by the characteristic bend in the DTG curves (according to the mass variation). Similar thermal decomposition processes occurred in the biochar-MH, biochar-300 and biochar-500 samples. The completion of the combustion of destructive residues in the biochar-MX sample within 346–443 °C, resulted in a mass loss of 18.2 %. The biochar-300 sample lost 27.3 % of its mass within 340–430 °C, and biochar-500 lost 28.6 % at 350–445°C.

At the fifth stage of thermolysis, in the temperature range of 423–650 °C, complete combustion of the pyrolytic residue of the initial raw material took place. This process was accompanied by a significant decrease in mass (31.9 %) and the appearance of a sharp exothermic effect on the DTA curve. The combustion of the pyrolytic residue from biochar-MX at the fourth stage of thermolysis (443–650 °C) was accompanied by a mass loss of 29.1 %. The biochar-300 sample lost 46.5 % of its

Journal of Chemistry and Technologies, 2026, *34*(2), 439-447

mass at 430–650°C, and biochar-500 lost 55.3 % from 445 to 690 °C. The combustion processes of destruction residues and pyrolytic residues in the studied biochar samples are characterised by greater mass loss and more pronounced exothermic effects on the DTA curves. This indicates a higher content of thermally stable components in these samples.

Additional data on the nature of chemical bonds in biochar and raw plant material were obtained using IR spectroscopic analysis. The IR spectrum of biochar (Fig. 3) shows a characteristic absorption band at 1168 cm^{-1}, which corresponds to skeletal vibrations. The absorption peak observed around 1616 cm^{-1} corresponds to vibrations of bonds in β-conformations, whereas the peak at 2314 cm^{-1} is attributed to symmetric vibrations of methyl groups. Absorption near 3305 cm^{-1} arises from vibrations of amino groups involved in hydrogen bonding, while a distinct peak at 3428 cm^{-1} reflects vibrations of free amino groups. Bands in the 2840–2900 cm^{-1} range indicate stretching vibrations of –CH and –CH_2– groups.

In the spectrum of the raw material (Fig. 4), absorption bands characteristic of sugars containing galactose units appear in the 700–900 cm^{-1} region. Additionally, bands corresponding to –SO_2–O– groups are observed, notably a doublet at 1260 and 1230 cm^{-1}, which arise from asymmetric stretching vibrations of O=S=O groups.

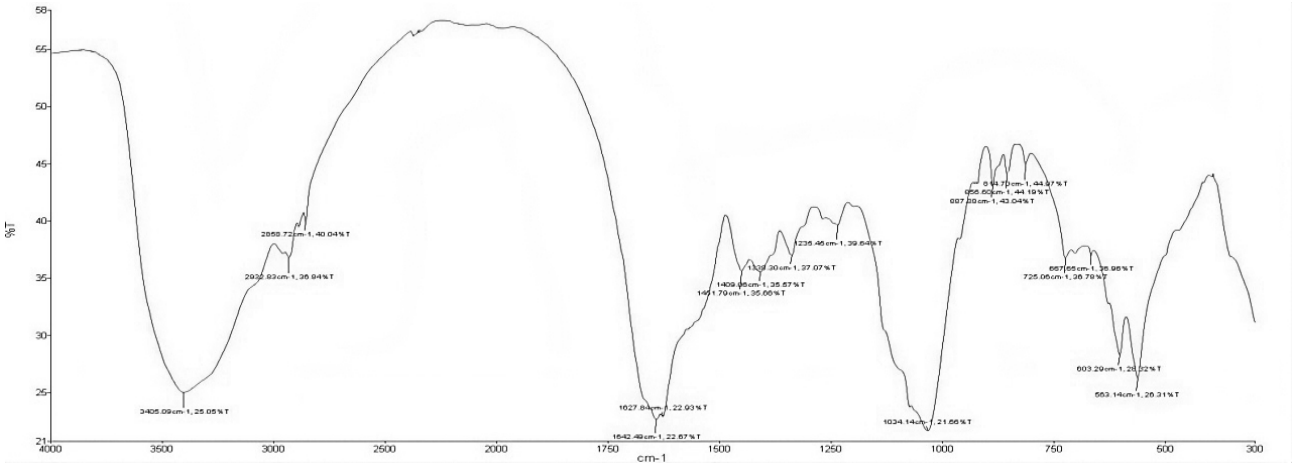

Fig. 3. Infrared spectrum of Biochar-300

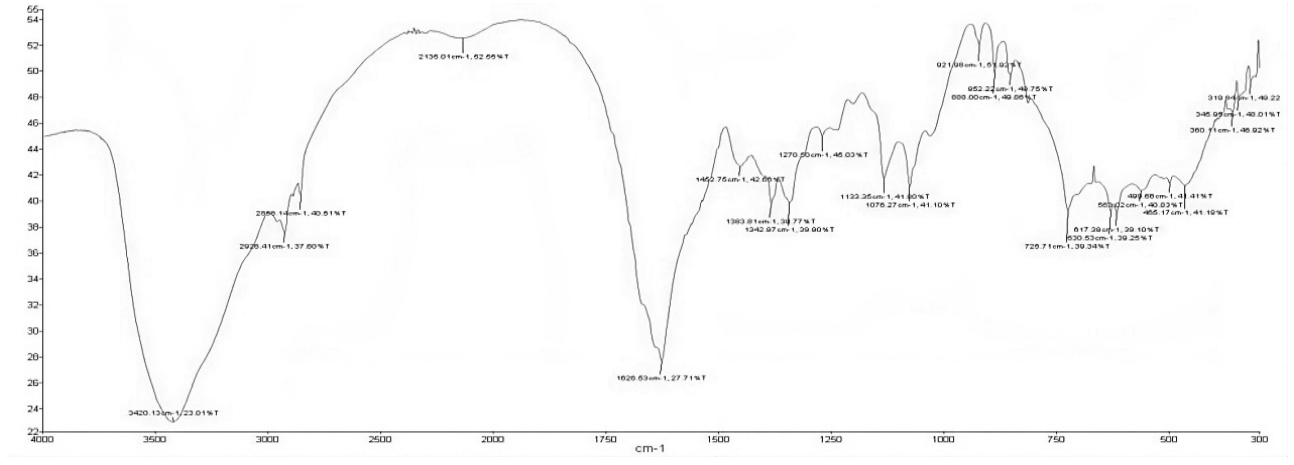

Fig. 4. Infrared spectrum of raw materials

The biochar spectrum exhibits a broad, intense band with a maximum at 3400 cm^{-1}, shifted to lower frequencies relative to free OH^- groups, indicating that hydroxyl groups are involved in hydrogen bonding [22]. The lack of a band at 3650 cm^{-1} suggests that nearly all hydroxyl groups participate in the hydrogen bond network. For a comparative analysis of the biochar and raw material samples, differential infrared spectroscopy was employed (Fig. 5).

Journal of Chemistry and Technologies, 2026, *34*(2), 439-447

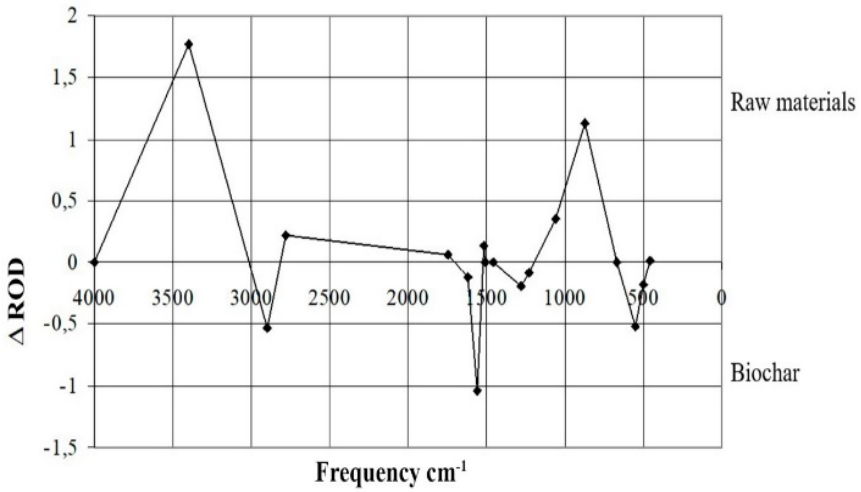

Fig. 5. Please insert here the figure caption

The comparative differential infrared spectrum of the raw material and biochar-300 (Fig. 5) reveals stronger absorption in the 670–1225 cm^{-1} region present in the raw material, due to amino group fragments in protein structures. The reduced relative optical density (ROD) observed for biochar-300 in the same spectral region likely reflects the degradation of protein components during heat treatment (pyrolysis). The differential spectrum comparing ROD values also shows a reduction in the absorption intensity of the raw material near 3400 cm^{-1}, associated with the stretching vibrations of free hydroxyl (OH^-) groups. This suggests enhanced intra- and/or intermolecular hydrogen bonding in the resulting biochar structure.

The surface characteristics of biochar, which determine its structural features, play a critical role in its functional properties. Therefore, these parameters require careful analysis. The measured values of average pore radius (r, $\times 10^{-10}$ m) and specific surface area (S_{sp}, m^2/g) are summarized in Table 2.

Table 2

Structural characteristics of the biochar surface

Sample	Structural characteristics of the surface	
	r*10¹⁰[m]	S_{sp} [m^2 /g sample]
Biochar-500	24.80	164.21
Biochar-300	27.01	132.77
Biochar-MX	26.99	152.19
Raw materials	26.98	130.07

The experimental data from a comparative analysis of the surface structure of biochar and its precursor materials, as summarized in Table 2, indicate that the surface area of biochar is considerably higher than that of the original raw materials. This demonstrates the effectiveness of the applied strategies for modifying the raw material to enhance its functional characteristics. Rising pyrolysis temperatures are associated with an increase in the specific pore surface. Notably, the highest surface area development was observed in the sample produced via microwave-assisted pyrolysis. This highlights the potential and practicality of employing this technique to produce biochar with superior functional properties suitable for applications in environmental technologies.

Conclusions

Comprehensive thermal analysis revealed that the thermodestruction processes of the raw plant material and the derived biochar follow similar stages; however, they differ significantly in the intensity of mass loss across specific temperature intervals. Biochar is characterized by a reduced content of thermolabile components (hemicellulose and partially cellulose), which is confirmed by lower mass losses in the 200–350 °C range.

It was established that increasing the pyrolysis temperature (from 300 to 500 °C) enhances the thermal stability of biochar. This is manifested by a shift of the main decomposition stages toward higher temperatures and an increase in the fraction of mass lost during the oxidation of the carbonaceous residue.

Despite differences in chemical composition and thermal behavior, the total mass loss of the raw material and biochar is comparable. This can be explained by the complete oxidation of the organic fraction of the samples at high temperatures and the formation of a mineral (ash) residue of similar mass.

FTIR spectroscopic analysis showed that pyrolysis leads to the degradation of protein and polysaccharide structures and the formation of a more condensed aromatic carbon matrix. This is evidenced by a decrease in the intensity of absorption bands characteristic of amino groups and carbohydrate fragments, as well as by the strengthening of intermolecular hydrogen bonding.

Analysis of textural characteristics demonstrated that pyrolysis promotes the development of a porous structure and an increase in the specific surface area of biochar. The highest surface area values are achieved at higher pyrolysis temperatures or when microwave treatment is applied, indicating the effectiveness of these methods for producing sorption-active materials.

Overall, the obtained results indicate that the thermal treatment of spent coffee grounds enables controlled modification of the structure, chemical composition, and functional properties of biochar, thereby confirming its potential for application in adsorption and environmental technologies.

References

[1] Björner Brauer, H., Hasselqvist, H., Måkansson, M., Willermark, S., Hiller, C. (2024). Re-configuring practices in times of energy crisis – A case study of Swedish households. *Energy Research & Social Science*, *114*, 103578. https://doi.org/10.1016/j.erss.2024.103578

[2] Faggian, L., Agostini, S., Müller, B., Gupte, A. P., Favaro, L. (2025). Efficient production of hydrogen through bioaugmentation of the organic fraction of municipal solid waste by the newly isolated Clostridium sartagoforme SA1. *Bioresource Technology*, *415*, 131658. https://doi.org/10.1016/j.biortech.2024.131658

[3] Sokolova, T., Krusir, G., Shunko, H., Korkach, H., Makarova, O., Tolstykh, V., Sokolova, V. (2024). Preparation and study of acid-base and ion-exchange properties of biochar from waste coffee grounds. *Ecological Engineering & Environmental Technology*, *25*(11), 399–409. https://doi.org/10.12912/27197050/193052

[4] Torboli, A., Foladori, P., Lu, M., Gialanella, S., Maines, L. (2024). Spent coffee ground biochar for phosphate adsorption in water: Influence of pyrolysis temperature and iron-coating activation method. *Cleaner Engineering and Technology*, *23*, 100839. https://doi.org/10.1016/j.clet.2024.100839

[5] Sharma, T., Hakeem, I. G., Gupta, B. A., Joshi, J., Shah, K., Vuppaladadiyam, A. K., Sharma, A. (2024). Parametric influence of process conditions on thermochemical techniques for biochar production: A state-of-the-art review. *Journal of the Energy Institute*, *113*, Article 101559. https://doi.org/10.1016/j.joei.2024.101559

[6] Premchand, P., Demichelis, F., Chiaramonti, D., Bensaid, S., Fino, D. (2022). Study on the effects of carbon dioxide atmosphere on the production of biochar derived from slow pyrolysis of organic agro-urban waste. *Waste Management*, *172*, 308–319. https://doi.org/10.1016/j.wasman.2023.10.035

[7] Skliar V., Krusir G., Zakharchuk V., Kuznecova I., Malovanyy M. (2020). Study of the physical and chemical characteristics of an immobilized lipase in the hydrolysis of fat waste. *Ecological Questions*, 31(3), 1644-7298. http://dx.doi.org/10.12775/EQ.2020.019

[8] Pambudi, S., Jongyingcharoen, J. S., Saechua, W. (2024). Thermochemical treatment of spent coffee grounds via torrefaction: A statistical evidence of biochar properties similarity between inert and oxidative conditions. *Results in Engineering*, *21*, 102012. https://doi.org/10.1016/j.rineng.2024.102012

[9] Kochito, J., Gure, A., Abdisa, N., Tadesse, B. T., Femi, O. E. (2024). Magnetic biochar nanocomposites of coffee husk and khat (Catha edulis) leftover for removal of Cr (VI) from wastewater. *Current Research in Green and Sustainable Chemistry*, *8*, Article 100403. https://doi.org/10.1016/j.crgsc.2024.100403

[10] Kupriyashkina H., Pylypenko L., Sevastyanova E., Mazurenko K, Hugi Ch., Breitenmoser L., Krusir G., Malovanyy M. (2024). Microbiological landscape of oil-contaminated soil and its bioremediation by microorganisms. *Ecological Engineering & Environmental Technology*, 25(2), 31–40. https://doi.org/10.12912/27197050/175139

[11] Gwenzi, W., Chaukura, N., Noubactep, C., Mukome, F. N. D. (2017). Biochar-based water treatment systems as a potential low-cost and sustainable technology for clean water provision. *Journal of Environmental Management*, *197*, 732–749. https://doi.org/10.1016/j.jenvman.2017.03.087

[12] Khomych G., Krusir G., Horobets O., Levchenko Y., Gaivoronska Z. (2020). Development of Resource Effective and Cleaner Technologies Using the Waste of Plant Raw Materials. *Journal of Ecological Engineering*, 21(4), 178–184. https://doi:10.12911/22998993/119814

[13] Soloviy, Ch., Malovanyy, M., Bordun, I., Ivashchyshyn, F., Borysiuk, A., Kulyk, Y. (2020). Structural, magnetic and adsorption characteristics of magnetically susceptible carbon sorbents based on natural raw materials. *Journal of Water and Land Development*, *47*(X–XII), 160–168. https://doi.org/10.24425/jwld.2020.135043

[14] Krusir, G., Zakharchuk, V., Sevastyanova, E., Pylypenko, L., Mazurenko, K. (2021). Isolation of lysozyme of Black Sea Mussel Mutilus galloprovincialis. *Journal of Chemistry and Technologies*, *28*(3), 269–277. https://doi.org/10.15421/jchemtech.v29i3.223378

[15] Krusir, G., Hugi, Ch., Breitenmoser, L., Sevastyanova, E., Pylypenko, L., Mazurenko, K. (2022). Isolation and characterization of a pancreatic amylase inhibitor. *Journal of Chemistry and Technologies*, *30*(4), 558–567. https://doi.org/10.15421/jchemtech.v30i4.263201

[16] Krusir G., Zakharchuk V., Sevastyanova E., Pylypenko L., Moshtakov S. (2020). Isolation of Alfalfa Seed Trypsin

Inhibitor using Affinity Chromatography. *Journal of Chemistry and Technologies*, 28(3), 269-277. https://doi.org/10.15421/08202803

[17] Sharma, A., Pareek, V., Zhang, D. (2015). Biomass Pyrolysis - A Review of Modelling, Process Parameters and Catalytic Studies. *Renewable and Sustainable Energy Reviews*, *50*(9), 1081–1096. https://doi.org/10.1016/j.rser.2015.04.193

[18] Cha, J., Park, S., Jung, S. C., Ryu, C., Jeon, J. K., Shin, M. C., Park, Y. K. (2016). Production and Utilization of Biochar: A Review. *Journal of Industrial and Engineering Chemistry*, *40*, 1–15. https://doi.org/10.1016/j.jiec.2016.06.002

[19] Yaashikaa, P. R., Kumar, P., Varjani, S., Anbalagan, S. (2019). Advances in production and application of biochar from lignocellulosic feedstocks for remediation of environmental pollutants. *Bioresource Technology*, *292*, 122030. https://doi.org/10.1016/j.biortech.2019.122030

[20] Yalechko, V., Kochubey, V., Hnatyshyn, Y., Pavlovskyi, Y. (2016). Thermal analysis of willow wood (Salix Viminalis). *Scientific Bulletin of UNFU*, *26*(4), 247–251. https://doi.org/10.15421/40260438

[21] Yang, H., Yan, R., Chen, H., Lee, D. H., Zheng, C. (2007). Characteristics of hemicellulose, cellulose and lignin pyrolysis. *Fuel*, *86*(12-13), 1781–1788. https://doi.org/10.1016/j.fuel.2006.12.013

[22] Krusir, G., Pylypenko, L., Sevastyanova, E., Mazurenko, K., Moshtakov, S., Shunko, H., Vitiuk, A., Shpyrko, T., Zdoryk, O. (2023). Isolation and characterization of pancreatic lipase inhibitor from rapeseed seeds. *Journal of Chemistry and Technologies*, *31*(2), 255–270. https://doi.org/10.15421/jchemtech.v31i2.279214